ANALYSIS OF COMPOSITE ADHESIVE-BONDED JOINTS

Libin ZHAO [a], Jiaxi LI [b], Tianliang QIN [c], Hai HUANG [d]
School of Astronautics, Beihang University, Beijing, 100191, PR China
[a] Lbzhao@buaa.edu.cn, [b] Lijiaxibuaa@sina.com, [c] qtl@tom.com, [d] hhuang@buaa.edu.cn

SUMMARY

A 3D FE analyses is created to understand the mechanics behaviour of composite π joint under pull-off load. Stress distributions of each part are discussed to disclose the load transfer path. Static tests were made to verify the numerical results. The results illustrate the triangle zone is the weakness and need to be paid more attention to.

Keywords: finite element analysis; composite ; adhesive-bonded joint; Static test; initial damage load

INTRODUCTION

Composites are commonly used because of their high strength and stiffness, low mass, excellent durability and ability to be formed into complex shapes. Nowadays new design concepts on non-plane joint are proposed [1-2] to cope with the requirements of integrated composite structure as primary aircraft structure. These all-composite joints connect the composite structures and can bring enormous potential benefits from the reduction of the fastener and the part count, which lead to the dramatic decrease of assemble cost and primary structural weight [2]. However, the connection of such joint represents a zone of potential weakness when the joint transmit tensile, bending and shear stresses between the different parts of the airplane and should be investigated deeply [3]. In the last twenty years, there is a large body of literatures to research the mechanics behaviour of out-of-plane composite tee-joint [3-12], single-L joint [13-14] and top-hat joint [15-17] by numerical and experimental method. However, at present there is no report on the stress distribution and the load transfer path of composite π joint.

In this paper, to provide deeply understand of the mechanics behaviour of composite π joint, a 3D FE numerical model is created by means of Software ABAQUS. The stress distribution of π shaped joints under tensile load is studied and load transfer path is described. The weak zone of composite π joint is determined. Furthermore, the numerical results are compared with experimental results.

STRUCTURE OF COMPOSITE π JOINT

A typical configuration of composite π joint is illustrated in Figure 1. The vertical web and the horizontal skin is connected by the π shaped overlaminate, which is made of double L prepregs, single U prepreg, double fillers and sometimes a base prepreg.

The all-composite π joint is made of high-tensile strength, uni-directional carbon fibre prepreg with a bismaleimide resin matrix. The web and skin are sandwich panels contains honeycomb. The joint is clamped on the two ends of the skin and subjected to a pull-off load on the top of the web, as shown in figure 2. The dimension and lay-ups of the several composite parts were as follows:

- Web: H×T×K=160×6.5×50mm, Stacking of both sides: [90°/-45°/0°/45°]s
- Skin: W×M×K=110×4×50mm, Stacking of up and bottom sides: [45°/90°/-45°/0°]s
- Base-prepreg: 67×0.36×50mm, Stacking: [-45°/90°/45°]
- L-prepreg: 30×24×0.36mm with a 3 mm internal radius, Stacking: [45°/90°/-45°]
- U-prepreg: 6.5×24×0.36mm with a 3 mm internal radius, Stacking: [45°/90°/-45°]

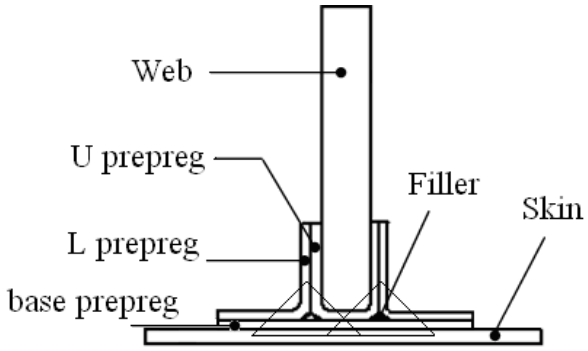

Figure 1 Configuration of composite π joint

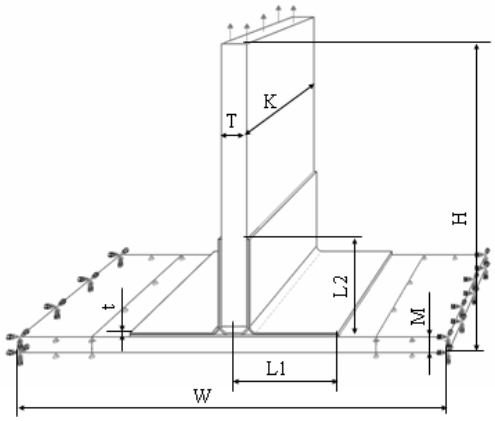

Figure 2 Load and constraints

3D NUMERICAL MODEL

A 3D FE analysis approach is used to investigate the stress distribution of the π joint. Based on the software ABAQUS, the FE model of composite π joint is carried out using eight-noded solid elements C3D8, C3D8R and six-noded solid element C3D6 with three displacement degrees of freedom per node. Each composite ply is set volume. The triangle zone, as shown in Figure1, is fine meshed. In view of the curved composite prepreg in the triangle zone, four local cylindrical coordinate systems are established to define material direction angles of composite lamina. Table 1 gives the material properties.

Table 1 Material properties

Elastic parameters	Unit	Value	Strength parameters	Unit	Value
E_1	GPa	121	X_t	MPa	2326
$E_2 = E_3$	GPa	7.46	X_c	MPa	1236
$\nu_{12}=\nu_{13}=\nu_{23}$	-	0.31	$Y_t = Z_t$	MPa	51
			$Y_c = Z_c$	MPa	209
$G_{12}=G_{13}= G_{23}$	GPa	5.18	$S_{12}= S_{13}$	MPa	87.9
			S_{23}	MPa	99.2

The linear elastic analysis is processed under an assumed pull-off load 5000N which is applied on the upper surface of web. The two ends of the skin are fixed only along vertical direction on the upper and bottom sides. However, the nodes on the two end edges are fixed in all the degree of freedoms. Thus the stress distribution trend can be obtained and the stress level and load carrying ability of different composite part in the π joint can be accessed.

STRESS DISTRIBUTION OF EACH COMPOSITE PART

The aim is to understand the stress distribution of each part (L prepreg, U pregreg, filler, base prepreg) under a total tensile load on the web. In view of the geometry complexity of the composite π joint, this is done by considering the calculated stress plots as a function of distance along defined paths, which are shown in figure 3. The L-path A-B-C-D is along the outer border of L prepreg. The U-path E-G-H-I-J-K is along the outer border of U prepreg. Base-path M-N-O-P-Q-R is along the upper line on the mid-width of base prepreg. And the filler-path S-T-W-S is closed along the border of the filler triangle.

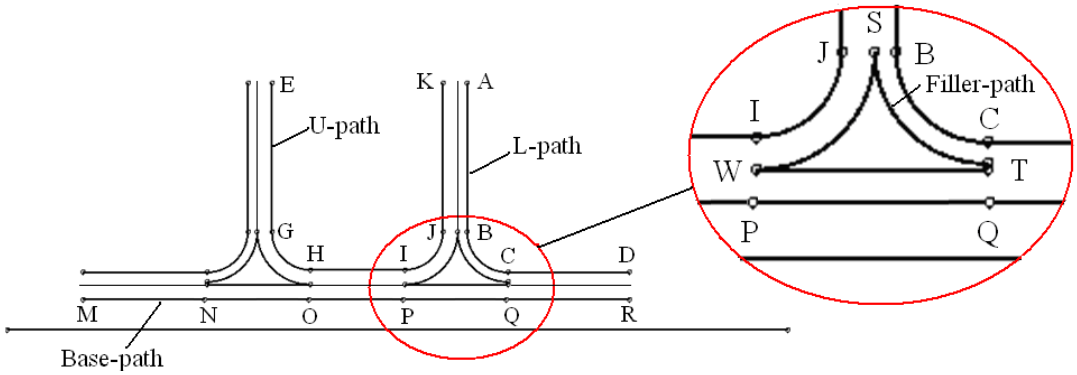

Figure 3 Sketch of paths

Figure 4 gives the stress curves of L prepreg along the path A-B-C-D. It can be seen that all stresses from A to B are very small, which illustrated there are little load transmitted by the vertical part of L prepreg. In the corner, i.e., between B and C on the path, there are almost zero stress along the fibre direction. In the plane of composite lamina, there are compressed stresses in the transverse direction vertical the fibre. At the same time, the in-plane shear, the out-plane shear and the interlaminate stress increase rapidly and thus the pull-off load from the web is mainly transferred by these stresses in the corner. In view of the strength parameters listed in Table 1, the shear and interlaminate stress should be paid more attention to. The horizontal part of the L prepreg, i.e., the curves between C and D on the path show that the interlaminate normal and shear stresses are very small whereas the in-plane stresses are gradually decreased along the path. In this part the load is mainly transferred by in-plane stresses.

Figure 5 shows the stress curves of U prepreg along the path E-G-H-I-J-K. From the figure it can be seen that normal stresses of each ply are symmetric about the midpoint of path H-I. In addition, the in-plane shear stresses σ_{12} are antisymmetric in the vertical part of U prepreg and symmetric in the curved and horizontal part. However, the out-of-plane shear stresses σ_{13} are symmetric in the vertical part of U prepreg whereas

antisymmetric in the curved and horizontal part. Furthermore, the out-of-plane shear stresses σ_{23} are completely antisymmetric about the midpoint of path H-I.

In the vertical part of the U prepreg, some of tensile loads from the web are mainly transferred by the shear stresses σ_{12} and σ_{13} of ±45° plies and the normal stress σ_{11} of 90° ply. But more loads are transmitted by the corner and the horizontal part of the U-prepreg with diverse stress styles.

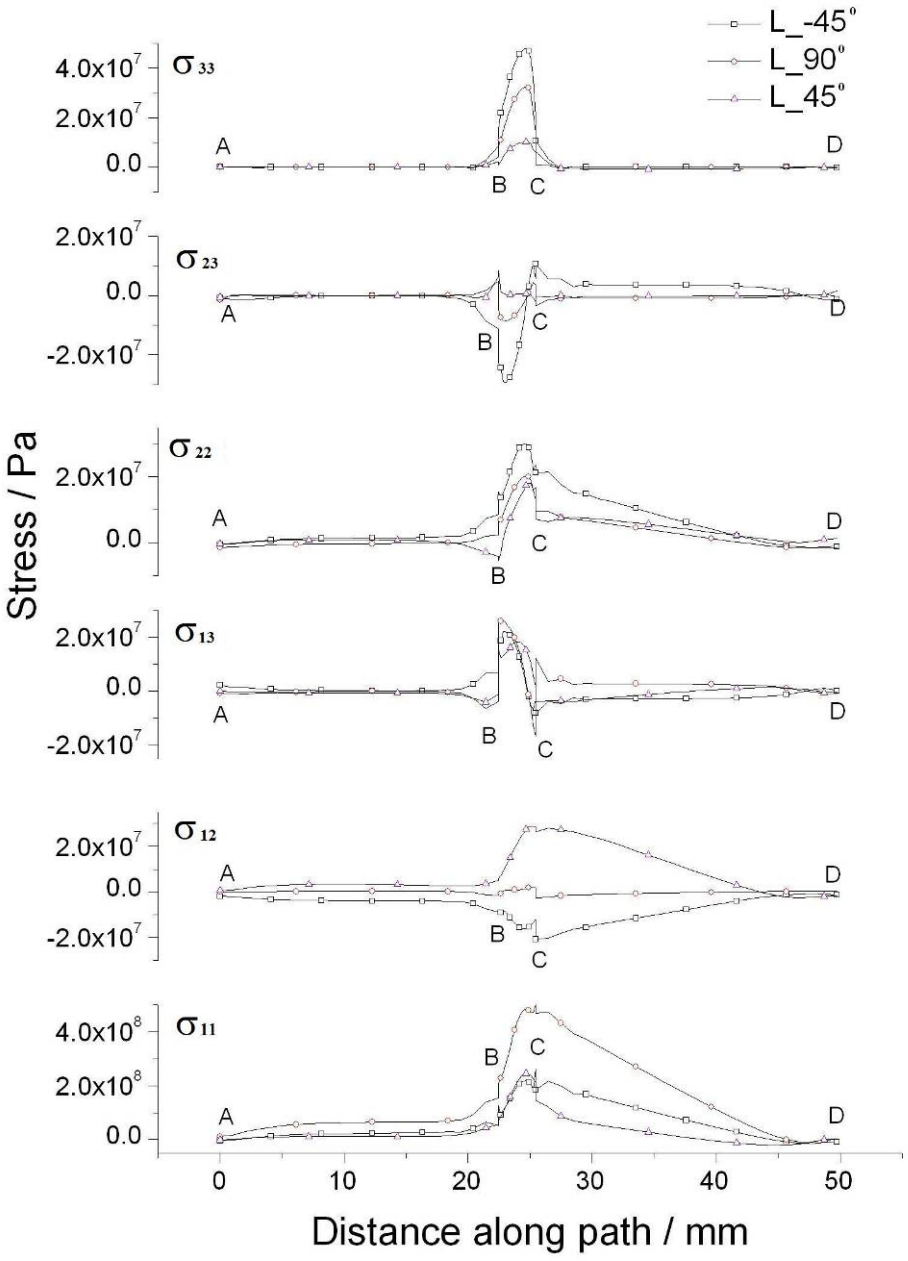

Figure 4 Stress distributions along L-path

At the same time, it is worth to note that the interlaminate normal and shear stress levels on the position G and J are very high. The two point connect the vertical parts and the corner parts of U prepreg. In view of the strength parameters shown in Table 1, these positions are critical during the load transfer and should be paid more attention to.

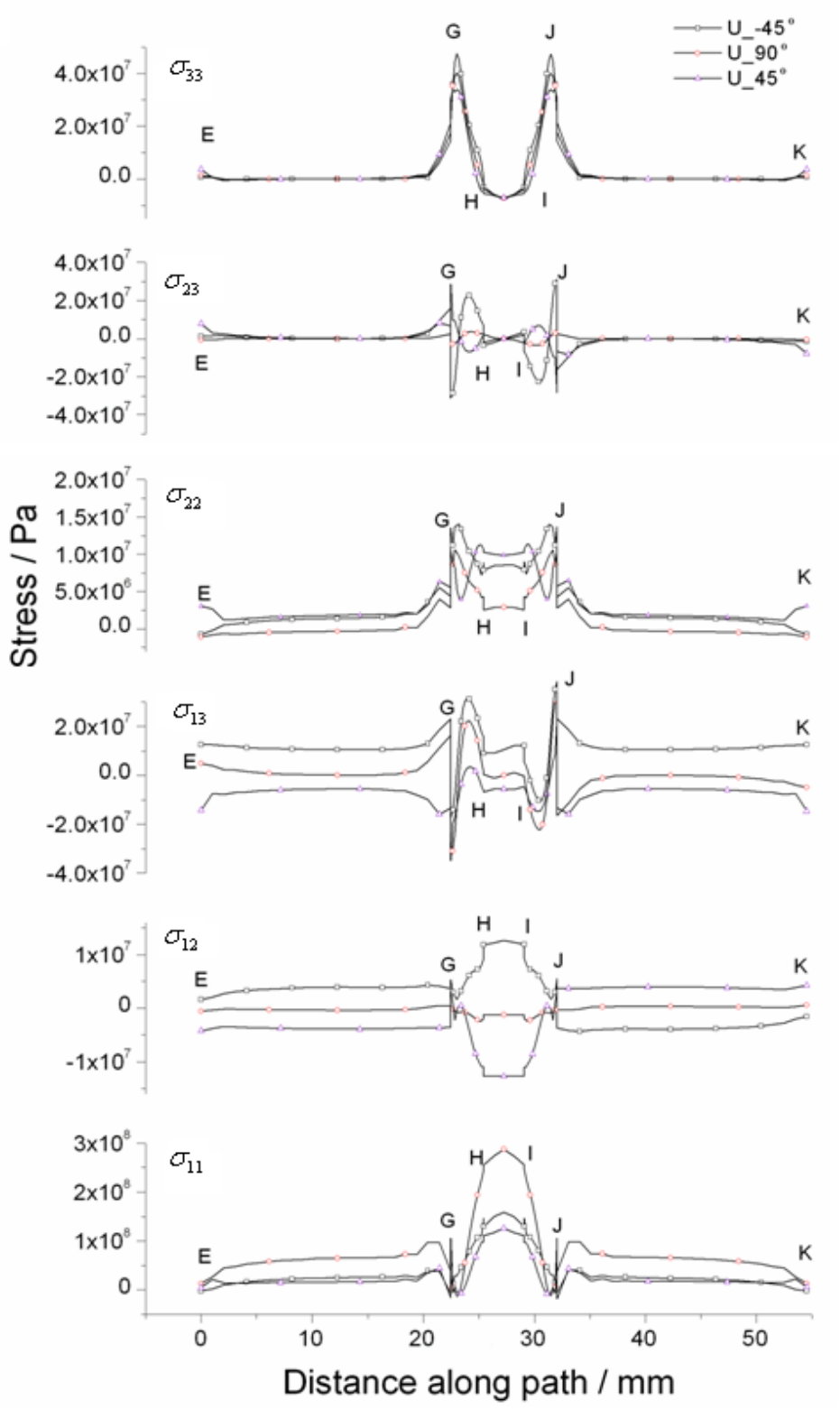

Figure 5 Stress distributions along U-path

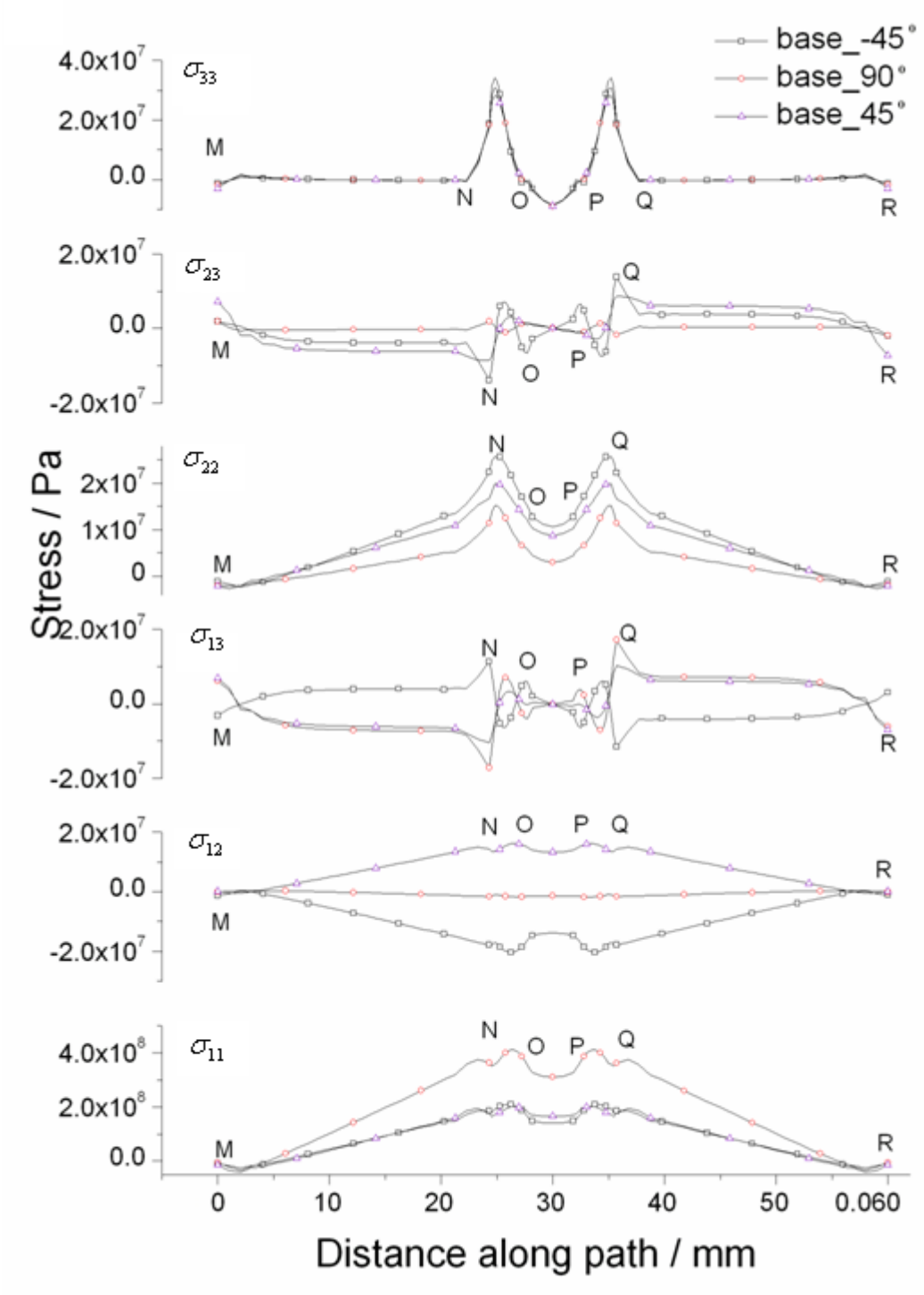

Figure 6 Stress distributions along Base-path

Fig.6 shows the stresses of base prepreg along the path M-N-O-P-Q-R. The normal stresses and the in-plane shear stress are symmetrical, whereas the out-plane shear stress are anti-symmetric about the midpoint of path O-P. It can be seen that the peak value of stresses located on the paths N-O and P-Q, which are under the fillers, and gradually decreased towards the two ends of the base prepreg. Thus the tensile load from the web is mainly transmitted through the filler and spread by the base prepreg.

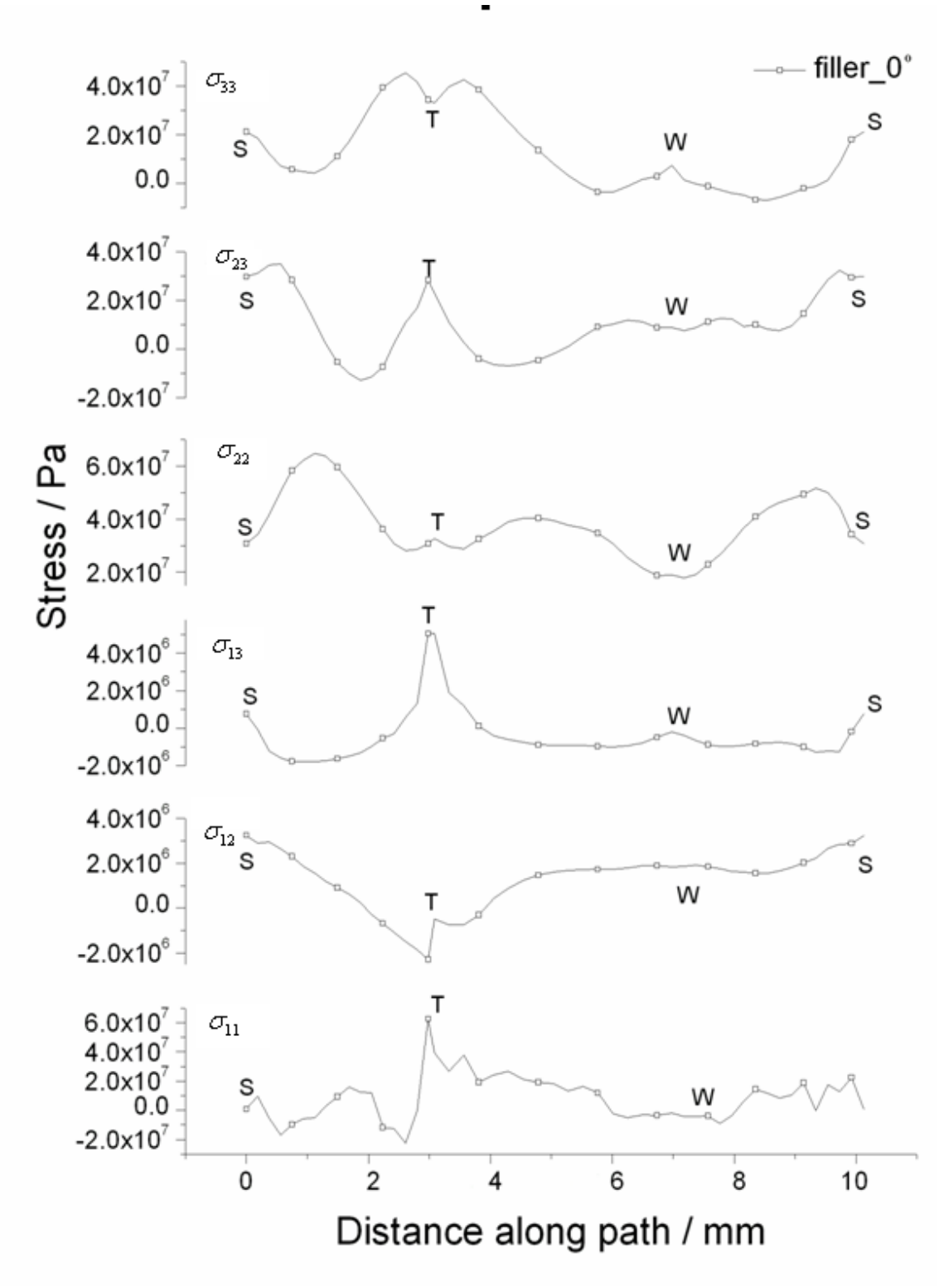

Figure 7 Stress distributions along Filler-path

Figure 7 shows the stresses along the path S-T-W-S. Compared with Fig.4 to Fig.6, the stresses level of σ_{11}, σ_{12} and σ_{13} are very small and about 1/10 of the corresponding stress levels of L, U and base prepreg. Thus the load is mainly transferred by σ_{22}, σ_{23} and σ_{33}. The peak value occurs on the path S-T (including S and T point) which

illustrated that the interface between the filler and the L prepreg, the position near S and T should be paid more attention to.

STRENGTH RATIO OF EACH COMPOSITE PART AND DISCUSSION

After getting the stress distribution, a failure criterion is needed to assess the structural integrity and determine which lamina may fail. In this paper a modified maximum stress failure criterion [18] is used to predict the damage onset of composite π joint. This criterion is based on the assumption that the composite lamina is transverse isotropic in the plane vertical to the fibre and can be described as follows:

$$\sigma_1 = X_t, \quad \sigma_{s1} = (\sigma_2 + \sigma_3)/2 + \sqrt{(\frac{\sigma_2 - \sigma_3}{2})^2 - \tau^2_{23}} = Y_t, \quad \tau_{12} = \tau_{13} = S \qquad (1)$$

The strength ratio curves along the forementioned paths are given in Figure 8-11. These figures show that the most critical zone is on the filler, on which the interface between the filler and L prepreg has the highest strength ratio 1.276. In view of the assumed pull-off load 5000N, the initial damage load would be predicted as 5000/1.276=3918.5N. The corner on -45° ply of L prepreg and the connecting position between the vertical and corner of -45° ply of U prepreg have higher strength ratio too. Fig.12 gives the strength ratio contour in the triangle zone which shows that the red region will be the damage onset.

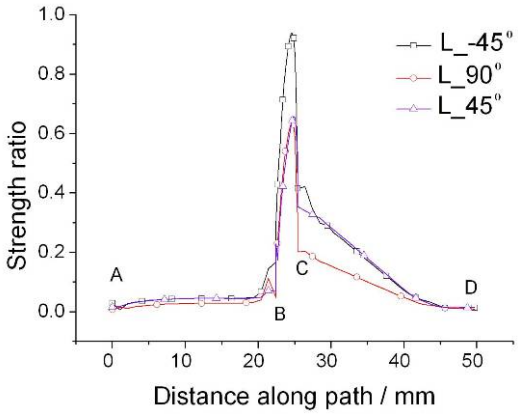

Figure 8 strength ratio along L-path

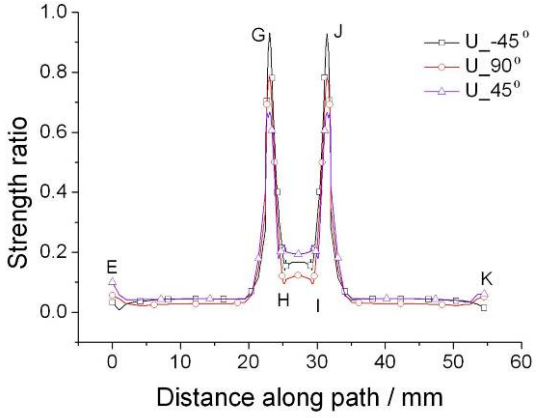

Figure 9 strength ratio along U-path

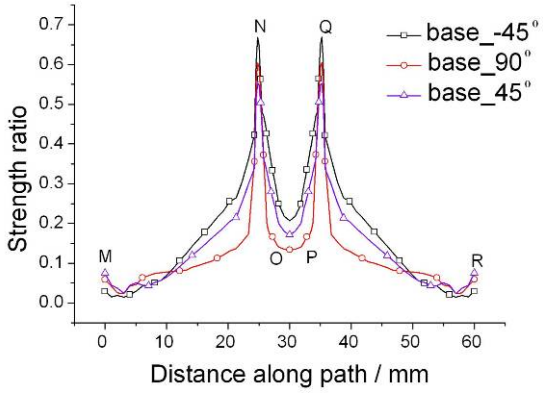

Figure 10 Strength ratio along base-path

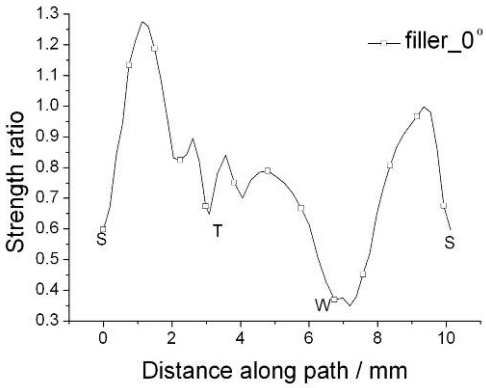

Figure 11 Strength ratio along filler-path

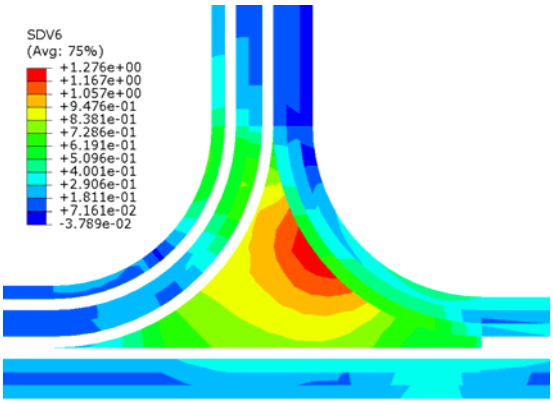

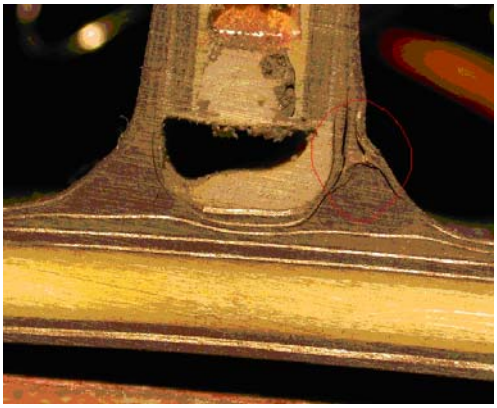

Figure 12 Strength ratio contour of triangle zone Figure 13 Damage status of the joint

EXPERIMENTAL RESULTS

Static tests were made in order to estimate the initial damage load resulting in onset of the damage and the ultimate failure load which can be applied to this joint. The average of initial damage load of five specimens is 4100N. Figure 13 shows the typical damage of one specimen. It can be seen that the filler is the weakness of the π joint.

CONCLUSION

A mechanics analyses was presented to predict the initial damage load of π-joint subjected to pull-off loading. The stresses along specified paths are given and the load carrying ability of each composite part is discussed. The stress results show that the corner of L prepreg, the connect position between the vertical part and corner of U prepreg, the corner of U prepreg, the filler near the corner of L prepreg, the two acmes of filler near L prepreg are all critical zone. Based on the modified maximum stress failure criterion, the strength ratio results show that the filler region near the corner of L prepreg has the highest strength ratio and will lead to the damage onset when the pull-off load arrives at 3918.5N. Compared with the experimental data of five specimens, the numerical prediction of damage initiation location is consistent with the experimental phenomena and the initial damage load error is equal to 4.4%, which illustrates the numerical analysis is effectively to predict structural initial damage under pull-off load.

References

1. Brian B. 41th AIAA/ASME/ASCE/ AHS/ASC Structures, April 2000, Atlanta.
2. Robert M. Taylor, Stephen D. Owens. 45th AIAA/ASME/ASCE Structures, April 2004.
3. J H Pei, R A Shenoi. Composite Part A (1996)89-103.
4. R A Shenoi, G L Hawkins. Composites 23(5): 335-345,1992
5. A R Rispler, G P Steven, L Tong. J Reinf. Plastic Compos. 16:1642-58, 1997
6. S Kumari, P K Sinha. J Reinf Plastic Compos. 21:1561-85, 2002

7. K Vijayaraju, P D Mangalgiri, B Dattaguru. Composite Structures 64:227-234, 2004
8. F Dharmawan, H C H Li, I Herszberg, S John. Composite Structures, 86:61-68, 2008
9. H C H Li, F Dharmawan, I Herszberg, S John. Compos Struct 75:339-350, 2006
10. E E Theotokoglou, T Moan. J Compos Mater, 30:190-209, 1996
11. U V R S Turaga, C T Sun. J Sandwich Struct Mater 2:225-45, 2000
12. H Toftegaard, A Lystrup. Compos A: Appl Sci Manufact, 36:1055-65, 2005
13. S Feih, H R Shercliff. Composites A: Appl Sci and Manufact. 36:381-395, 2005
14. S Feih, H R Shercliff. Int. J. of Adhesion and adhesives, 25:47-59, 2005
15. R A Shenoi, G L Hawkins. Composite structures, 30: 109- 121, 1995
16. J R House. Proc.ICCM-11, Gold Coast,vol. VI, 74–83, July 1997, Australia
17. J I R Blake, R A Shenoi, J House, T Turton. Ocean Engineering, 29:849–869, 2002
18. Libin Zhao, Tianliang Qin, Hai Huang, etc. Rare Metal Materials and Engineering, 2009. (in press)

Previous Paper ***Back to Programme*** ***Back to Topic*** *Next Paper*